Since January 2020 Elsevier has created a COVID-19 resource centre with free information in English and Mandarin on the novel coronavirus COVID-19. The COVID-19 resource centre is hosted on Elsevier Connect, the company's public news and information website.

European Journal of Medicinal Chemistry 225 (2021) 113766

Contents lists available at ScienceDirect

European Journal of Medicinal Chemistry

journal homepage: http://www.elsevier.com/locate/ejmech

Design, synthesis and structure-activity relationship studies of 4-indole-2-arylaminopyrimidine derivatives as anti-inflammatory agents for acute lung injury

Tianpeng Chen [a, 1], Yingying Wei [b, 1], Gaoyang Zhu [a], Huajun Zhao [b, **], Xingxian Zhang [a, *]

[a] College of Pharmaceutical Sciences, Zhejiang University of Technology, Hangzhou 310014, PR China
[b] School of Pharmaceutical Sciences, Zhejiang Chinese Medical University, Hangzhou, Zhejiang 311402, PR China

ARTICLE INFO

Article history:
Received 4 June 2021
Received in revised form
3 August 2021
Accepted 6 August 2021
Available online 12 August 2021

Keywords:
Acute lung injury
Anti-inflammatory
4-Indolyl-2-arylaminopyrimidine
Structure activity relationship
HBE cells

ABSTRACT

Acute lung injury/acute respiratory distress syndrome (ALI/ARDS), a clinically high mortality disease, has not been effectively treated till now, and the development of anti-acute lung injury drugs is imminent. Acute lung injury was efficiently treated by inhibiting the cascade of inflammation, and reducing the inflammatory response in the lung. A series of novel compounds with highly efficient inhibiting the expression of inflammatory factors were designed by using 4-indolyl-2-aminopyrimidine as the core skeleton. Totally eleven 4-indolyl-2-arylaminopyrimidine derivatives were designed and synthesized. As well, the related *anti*-ALI activity of these compounds was evaluated. Compounds **6c** and **6h** showed a superior activity among these compounds, and the inhibition rate of IL-6 and IL-8 release ranged from 62% to 77%, and from 65% to 72%, respectively. Furthermore, most of compounds had no significant cytotoxicity in *vitro*. The infiltration of inflammatory cells into lung tissue significantly reduced by using compound **6h** (20 mg/kg) in the ALI mice model, which achieved the effect of protecting lung tissue and improving ALI. In addition, the inflammatory response was inhibited by using compound **6h** through inhibiting phosphorylation of p-38 and ERK in MAPK signaling pathway, and resulted in protective effect on ALI. These data indicated that compound **6h** showed good anti-inflammatory activity *in vitro* and *in vivo*, which was expected to become a leading compound for the treatment of ALI.

1. Introduction

Acute lung injury (ALI) is a common complication of sepsis in intensive care unit patients. Although there are several treatment strategies of ALI, such as fluid management and protective ventilation, the high mortality rate is still existed due to the lack of effective drugs [1]. Studies have reported that pro-inflammatory and anti-inflammatory cytokines, including IL-1, IL-6, IL-8 and TNF-α, were related to the pathogenesis of inflammatory lung injury such as sepsis, pneumonia, aspiration, and shock [2]. Therefore, it's still urgent to develop novel and highly effective anti-inflammatory drugs for the treatment of ALI.

Epidermal growth factor receptor (EGFR) is a transmembrane glycoprotein in the ErbB tyrosine kinase receptor family. Currently, three generations of EGFR-tyrosine kinase inhibitors (TKIs) have been developed and approved for the treatment of advanced NSCLC patients with EGFR activating mutations [3]. Although EGFR inhibitors have made a lot of progress in anti-tumor, there were few studies on their use in the treatment of inflammatory diseases, such as ALI (Fig. 1). In 2011, Harada et al. showed that, the EGFR inhibitor gefitinib treatment prolonged inflammation and aggravated ALI in a naphthalene-induced lung injury model [4]. Liang Guang et al. reported that EGFR inhibitors AG1478 inhibited LPS-induced cell inflammation and significantly reduced LPS-induced ALI, which provided a strategy for the treatment of patients suffering from ALI induced by microbial infection [5].

Inhibition of EGFR provided a treatment plan for ALI caused by microbial infection [5]. In addition, Zhang et al. also reported that erlotinib reduced inflammatory response and reduced alveolar and vascular permeability by inhibiting EGFR and NF-κB signaling pathways, thereby protecting LPS-induced ALI [6]. Recently, Roh's research group reported that EGFR inhibitor **I**, based on pyrimidine

* Corresponding author.
** Corresponding author.
E-mail address: zhangxx@zjut.edu.cn (X. Zhang).
[1] The authors (Tianpeng Chen) and (Yingying Wei) are the co-authors.

https://doi.org/10.1016/j.ejmech.2021.113766
0223-5234/

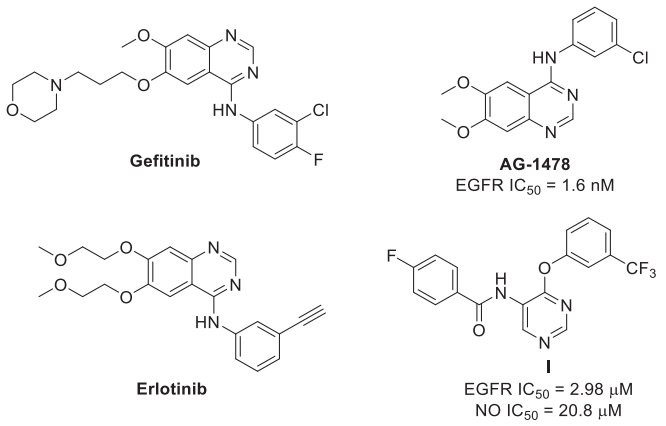

Fig. 1. EGFR small molecule protein kinase inhibitors.

skeleton modification, inhibited LPS-induced iNOS expression and the production of IL-1β, IL-6, and TNF-α in peritoneal macrophages (Fig. 1) [7]. The inhibitor weakened the activation of NF-κB through dephosphorylation of p65, inhibited the production of a variety of inflammatory factors, and thus exerted an anti-inflammatory effect. Therefore, the structural modification and transformation EGFR inhibitors were selected as a lead compound for the treatment of LPS-induced inflammation and ALI.

Many compounds containing indole skeleton and pyrimidine skeleton exhibited good anti-inflammatory activity [8]. Here, we assumed that combined indole and pyrimidine skeleton of **AZD-1,** an intermediate of the EGFR inhibitor osimertinib, had certain anti-inflammatory activity. Hence, we reported the design, synthesis and anti-inflammatory evaluation of 4-indole-2-arylami nopyrimidine derivatives (Fig. 2). By retaining 4-indole-2-arylaminopyrimidine nucleus of **AZD-1**, the replacement of fluorine atom with various amino substituents at 4-position of phenyl ring was firstly carried out based on classical drug design principles, the minimum change principle and bioisosterism, which could improve the hydrophilicity to enhance the biological activity of the compounds [9]. Secondly, the amino group at 5-position of phenyl ring was structurally modified by amidation reaction. Then, an azido group was allowed to be introduced, which has potent biological activity and could be readily functionalized. The structure-activity relationship of chain length lays a structural foundation for subsequent pharmacophore splicing and construction of nitrogen-containing heterocyclic derivatives [10,11]. We have synthesized twelve compounds, which contained 4-indolyl-2-arylaminopyrimidine structure. Furthermore, the inhibitory effect against LPS-induced IL-6 and IL-8 production in human bronchial epithelial (HBE) cells was evaluated. A series of compounds with various substitution on 4-position of phenyl ring group showed better activity than indomethacin at a concentration of 5 μM. Compound **6h** showed the highest anti-inflammatory activity. Further, we tested the effect of compound **6h** in the ALI model induced by LPS.

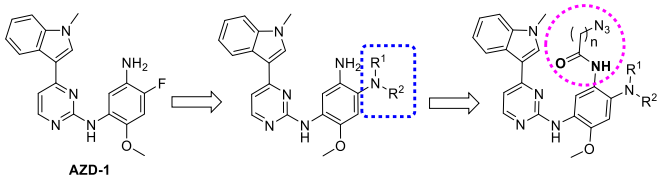

Fig. 2. Design of 4-indolyl-2-arylaminopyrimidine compounds.

2. Results and discussion

2.1. Chemistry

The synthetic route of 4-indolyl-2-arylaminopyrimidine derivatives is shown in Scheme 1. 2,4-Dichloropyrimidine **1** was treated with 1-methylindole in the presence of $AlCl_3$ to yield compound **2** [12]. The key intermediate **3** was synthesized from compound **2** via aromatic amination on the 2-position of pyrimidine, following reduction of nitro group to obtained **AZD-1**. Compounds **4a-h** were prepared by nucleophilic substitution of the key intermediate **3** with various aliphatic secondary amines. The desired compounds hydrochloride **6a-h** were provided by reduction of nitro group followed by treatment with HCl gas in EtOH. Furthermore, compound **5h** was reacted with various acyl chlorides to obtain **7a-b**. Subsequently, compounds **7a-b** were allowed to undergo nucleophilic substitution with sodium azide to produce compounds **8a-b**.

Reagents and conditions: (a) $AlCl_3$, DME, 80 °C; (b) *p*-TsOH•H_2O, 1,4-dioxane, 105 °C; (c) Fe, NH_4Cl, EtOH/H_2O, 100 °C; (d) various secondary amines, K_2CO_3, DMSO, 90 °C; (e) EtOH/HCl, r. t.; (f) various acyl chlorides, DCM, 0 °C-r.t.; (g) NaN_3, DMF, 90 °C

2.2. Anti-inflammatory screening and cytotoxicity of 4-indolyl-2-arylamino pyrimidine derivatives

The inflammatory cascade triggered by lung injury involves the activation of inflammatory cells and the release of mediators [13,14]. IL-6 and IL-8, two most important mediators of inflammation, have been extensively studied, which have been shown to be elevated in both plasma and BALF in patients with ARDS [15,16]. In order to explore the anti-inflammatory activity of 4-indolyl-2-arylaminopyrimidine derivatives, the production of IL-6 and IL-8 induced by LPS was determined in HBE cells. The aromatic nitro group should be avoided due to its potential to cause toxicity [17]. Therefore, the nitro-reduced derivatives **6a**-**6h** were preferably chosen to test the anti-inflammatory activity. In addition, in order to explore the structure-activity relationship of the substituents at 5-position of the phenyl ring, the nitro compound **4h** was selected as a control to compare the anti-inflammatory activity of **4h** and **5h**. Based on the optimal structure at 4-position of phenyl ring, the amino group at 5-position was structurally modified, which further produce the azide derivatives **8a**-**8b**. The anti-inflammatory activity of all synthesized compounds at concentration of 5 μM was evaluated by enzyme-linked immunosorbent assay (ELISA) *in vitro*. The inhibitory activities of twelve 4-indolyl-2-arylam nopyrimidine compounds on the release of IL-6 and IL-8 in LPS-induced HBE cells were shown in Fig. 3 and Fig. 4. The results indicated that most of the compounds have varying degrees of inhibitory effects on LPS-stimulated HBE cells. The lead compound AZD-1 had an inhibition rate of 63% and 49% for IL-6 and IL-8, respectively. Amino substituted derivatives 6a-6h on 4-position of phenyl ring showed better anti-inflammatory activity than indomethacin at concentration of 5 μM. Among them, Compounds 6c, 6f, and 6h showed excellent anti-inflammatory activity, and the inhibitory levels against the release of IL-6 and IL-8 were 62−77% and 65−87%, respectively. As well, the α-azido substituted amides 8a-b derived from 6h showed good inhibitory activity on the release of IL-6 and IL-8.

Before further studies, the cytotoxicity and safety of 4-indolyl-2-arylaminopyrimidine derivatives were evaluated in HBE cells by MTT assays at concentration of 10 μM (Fig. 5). Compared with the blank control, the cell survival rate of the lead compound **AZD-1** had no difference, indicating that there was no obvious cytotoxicity. Except for the potential cytotoxicity of compounds **4h** and **6f** to HBE

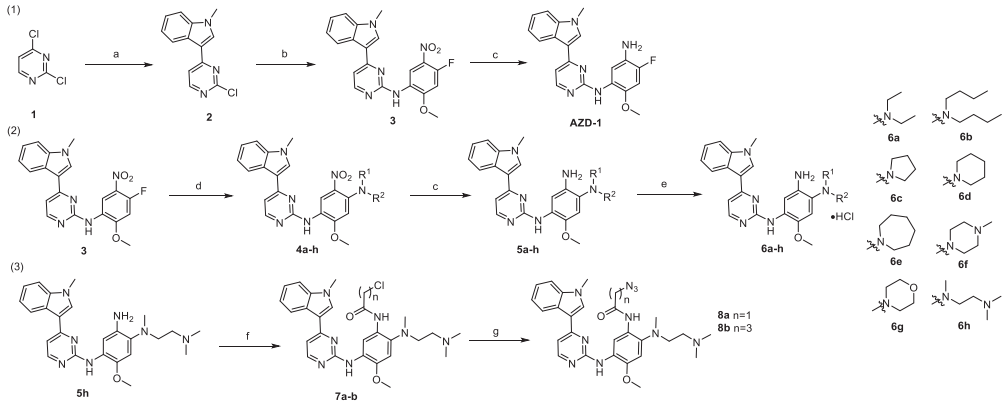

Reagents and conditions: (a) $AlCl_3$, DME, 80 °C; (b) p-TsOH•H_2O, 1,4-dioxane, 105 °C; (c) Fe, NH_4Cl, EtOH/H_2O, 100 °C; (d) various secondary amines, K_2CO_3, DMSO, 90 °C; (e) EtOH/HCl, r.t.; (f) various acyl chlorides, DCM, 0 °C-r.t.; (g) NaN_3, DMF, 90 °C

Scheme 1. Synthetic route of 4-indolyl-2-arylaminopyrimidine derivatives.

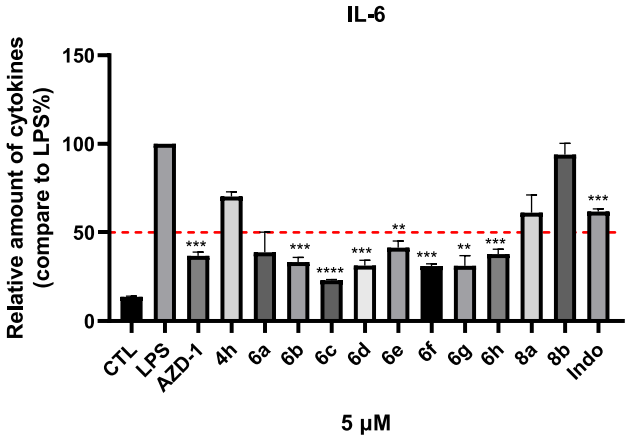

Fig. 3. Inhibitory activity of 4-indolyl-2-arylaminopyrimidine derivatives on the release of inflammatory cytokine IL-6.

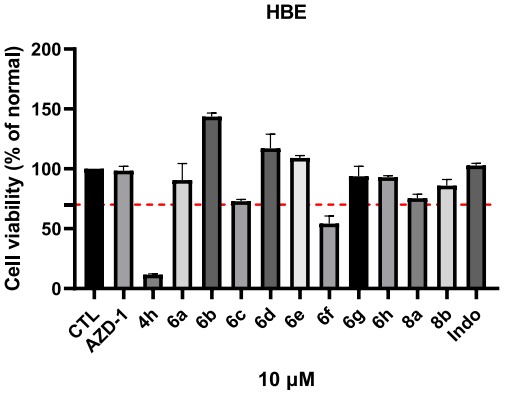

Fig. 5. Cytotoxicity evaluation of 4-indolyl-2-arylaminopyrimidine derivatives on HBE cell.

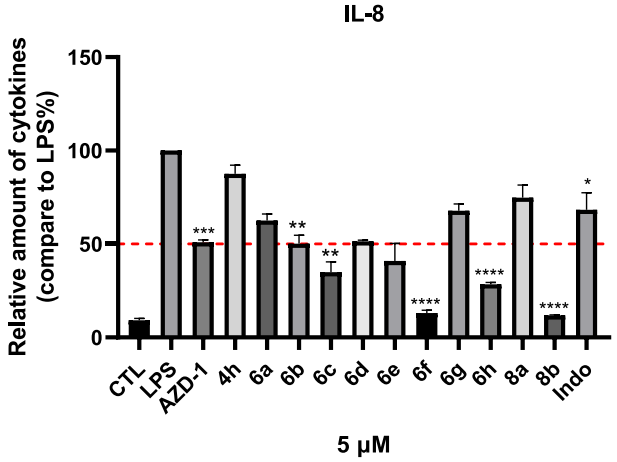

Fig. 4. Inhibitory activity of 4-indolyl-2-arylaminopyrimidine derivatives on the release of inflammatory cytokine IL-8.

cells (survival rates < 70%), other derivatives showed no obvious cytotoxicity, which preliminarily indicated that these compounds had certain safety *in vitro* and laid a foundation for subsequent activity evaluation *in vivo*.

2.3. Structure-activity relationship (SAR) of 4-indolyl-2-arylamino pyrimidine derivatives

Based on the results of anti-inflammatory screening experiments, we preliminarily summarized the structure-activity relationship (SAR) of 4-indolyl-2-arylamino pyrimidine derivatives (Fig. 6). Compounds **6a**-**6h** bearing amino substitution on 4-position of phenyl ring had a significant effect on anti-inflammatory activity compared to **AZD-1**. The summary is described as follows: (1) For open-chain aliphatic amines, the anti-inflammatory activity increased with the extension of chain length. The anti-inflammatory activity of compound **6b** containing dibutylamino group was significantly better than that of compound **6a** containing diethylamino group. (2) For cyclicaliphatic amino substituents, the smaller ring, the better anti-inflammatory activity. The inhibitory activity of compound **6c** containing tetrahydropyrrolyl substituent on IL-6 and IL-8 were better than that of compound **6d** bearing piperidinyl substituent and compound **6e** containing homopiperidinyl substituent. (3) For aliphatic amines containing two heteroatoms, the anti-inflammatory activity was

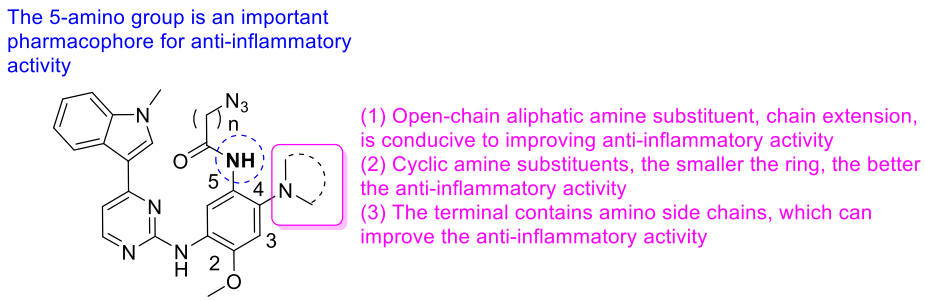

Fig. 6. Structure-activity relationship of 4-indolyl-2-arylaminopyrimidine derivatives.

enhanced when the terminal was an amino substituent. The activity of compound **6f** substituted by *N*-methylpiperazine and **6h** containing *N,N,N′*-trimethylethylenediamine was better than that of compound **6g** with morpholine substituent, respectively. Furthermore, the anti-inflammatory activity of compound **6f** with methylpiperazinyl group was better than that compound **6h** with *N,N,N′*-trimethylethylenediamine group. Obviously, cyclic aliphatic amines were more active than open-chain aliphatic amines.

The amino group on 5-position of phenyl ring played a vital role in anti-inflammatory activity. The comparison of the activity data of compounds **4h** and **6h** showed that the activity would be reduced when the amino group was changed to be nitro group. It indicated that the amino group may be an important pharmacophore and played an important role in maintaining anti-inflammatory activity.

The activity data of compounds **8a-b** preliminarily showed that the chain length between amido group and azido group had significantly affected on the anti-inflammatory activity. Compound **8b** with three-carbon chain length exhibited excellent inhibitory activity against IL-8, with an inhibition rate of 88%. However, compound **8a** with one-carbon chain length showed poor inhibitory activity against IL-6 and IL-8. Moreover, Compound **8b** has no obvious cytotoxicity.

2.4. Compounds **6h** ameliorate histopathological changes in lung tissues of LPS-induced ALI

After screening the anti-inflammatory activity and cytotoxicity, the compound **6h** showed better bioactivity *in vitro*. To further investigate the protective effect of **6h** by LPS-induced ALI, the pathological changes of lung tissues were studied (Fig. 7). The results of lung H&E staining showed that there were a large number of inflammatory cell infiltrates in the lung tissues of mice in the LPS group, accompanied by edema and destruction of the alveolar structure. Compound **6h** reduced inflammatory cell infiltration and edema in lung tissue of mice, and improved alveolar structure, especially the protective effect of **6h** (20 mg/kg) was more obvious. As a further evaluation, the lung Wet/Dry ratio (W/D) increased in mice with ALI. As shown in Fig. 8A, LPS significantly increased the wet to dry/gain ratio of the lung, while compound **6h** (10 mg/kg and 20 mg/kg) significantly decreased the wet to dry/gain ratio, indicating that compound **6h** reduced pulmonary edema. Bronchoalveolar lavage fluid (BALF) examination showed that compound **6h** (10 mg/kg and 20 mg/kg) reduced the total cell count in BALF (Fig. 8B). Total protein content in BALF significantly reduced in the **6h** administration group compared with the LPS group (Fig. 8C). These results indicated that compound **6h** significantly inhibited cell infiltration in lung tissue. Finally, these results indicated that compound **6h** had a good protective effect on LPS-induced acute lung injury in mice.

2.5. Compounds **6h** attenuated lung inflammation in LPS-induced ALI mice

The release of inflammatory cytokines played a key role in the development of ALI. As shown in Fig. 9, the LPS group significantly increased the mRNA expression of inflammatory cytokines (such as IL-1β, IL-6, and TNF-α) in lung tissue. However, compound **6h** administration reduced the release of inflammatory cytokines, especially the expression of IL-1β, IL-6 and TNF-α were significantly inhibited by compound **6h** (20 mg/kg). In addition, LPS stimulated the expression of inducible NO synthase (iNOS), promoted the synthesis of a large number of NO, and further aggravated the damage of lung tissue. Therefore, inhibiting the over-expression of iNOS played a protective role in ALI. Fig. 9D showed that the expression of iNOS in lung tissue of LPS group was significantly higher than that of control group, and the activity of iNOS could be significantly reduced by different doses administration of **6h**. These results indicated that compound **6h** inhibited the release of inflammatory cytokines and iNOS, and played a protective and therapeutic role in ALI of mice. As an effective anti-inflammatory small molecule, compound **6h** needs to be further developed for the treatment of ALI and other inflammatory diseases.

2.6. Inhibition of LPS-induced ERK and P38 signaling activation

Mitogen-activated protein kinases (MAPKs) pathway, composed of ERK, *c*-Jun amino-terminal kinases (JNK) and p38, was one of the key signaling pathways in the release of inflammatory cytokines stimulated by LPS [18]. The release of inflammatory mediators can be regulated through activation of MAPK signaling pathways,

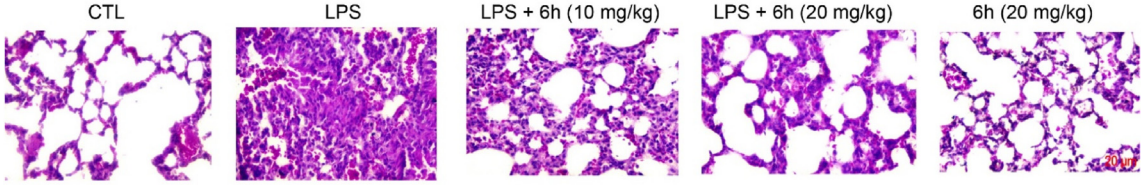

Fig. 7. Compound 6h ameliorate histopathological changes of lung in LPS-induced ALI mice.

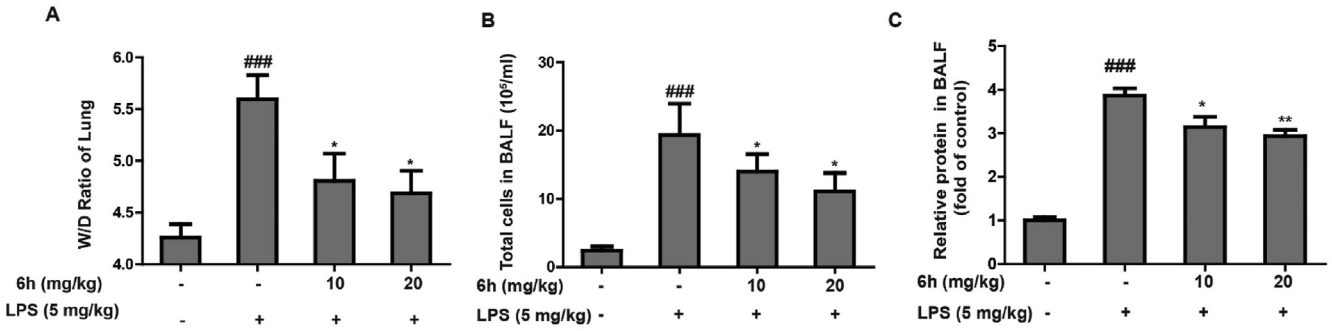

Fig. 8. Changes of lung wet-dry-weight ratio, total cell count and total protein content in alveolar lavage fluid.

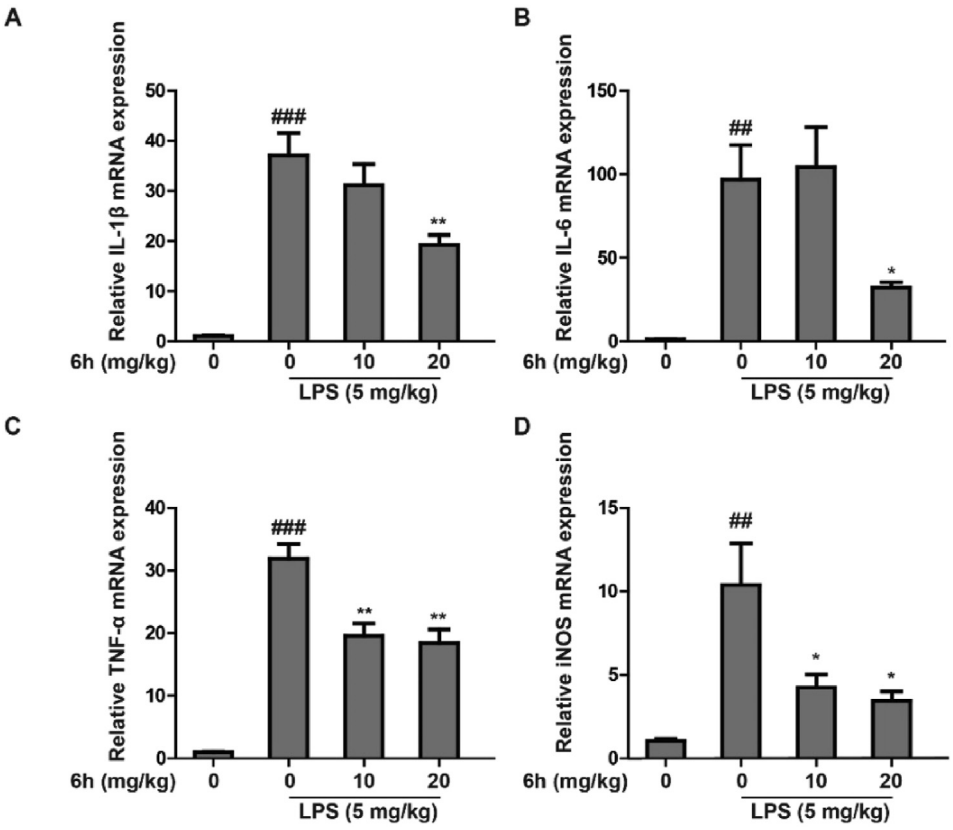

Fig. 9. Compound 6h attenuated lung inflammation in LPS-induced ALI mice.

especially p38 and ERK [19]. The possible mechanism of the anti-inflammatory activity of the compound **6h** *in vivo* was explored by studying the MAPK signaling pathway. As shown in Fig. 10, **6h** (20 mg/kg) significantly reduced phosphorylation of p38 and ERK. These results demonstrated that **6h** exerted an anti-inflammatory effect *in vivo* by suppression of MAPK signaling pathway.

2.7. Compounds 6h and 6c inhibit the phosphorylation level of EGFR

Finally, we further characterized the potential of compounds **AZD-1**, **6c**, and **6h** to inhibit EGF receptor and its phosphorylation by Western blotting analysis. It can be seen from Fig. 11 that **AZD-1**, **6c** and **6h** significantly inhibit the phosphorylation of EGFR in HBE cells. These results indicate that the structural modification and transformation of EGFR inhibitors can be used in the treatment of acute lung injury, and further indicate that EGFR may be a potential target for inflammatory diseases such as acute lung injury.

3. Conclusion

In this study, eleven compounds were designed and synthesized as anti-inflammatory candidate compounds using **AZD-1** as a lead compound, their cytotoxicity and *in vitro* and *in vivo* activities were evaluated as well. *In vitro* activity studies, most of them showed some degrees of anti-inflammatory activity. At the concentration of 5 μM, the lead compound **AZD-1** showed certain anti-inflammatory activity, inhibiting IL-6 and IL-8 by 63% and 49%, respectively. Among them, eight compounds containing amino substitution on 4-position of phenyl ring showed better anti-inflammatory activity than indomethacin. Especially, **6h** showed excellent inhibitory levels of IL-6 and IL-8 at 62% and 72%, respectively. In addition, azido-substituted amide derivative **8b** showed good inhibitory

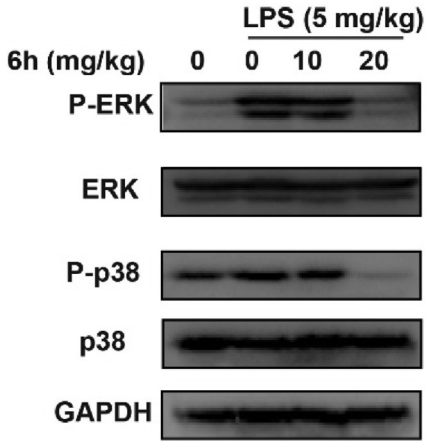

Fig. 10. Phosphorylation levels of ERK and p38 in MAPK pathway.

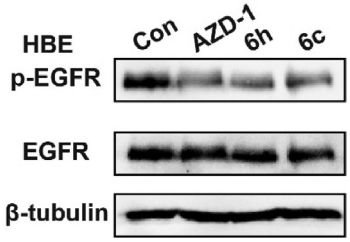

Fig. 11. Compounds **6h** and **6c** inhibit the phosphorylation level of EGFR.

activity against IL-8. MTT test showed that most of compounds have no potential cytotoxicity on HBE cells except **4h** and **6f**. The *anti*-ALI activity of the compound **6h** *in vivo* showed that it could significantly reduce the infiltration of inflammatory cells to lung tissue, reduce the inflammatory response and pathological changes in the lung, and thus play a protective role against ALI. Molecular mechanism experiments preliminarily confirmed that the compound **6h** inhibited the expression of various inflammatory factors, protected lung tissues and improved ALI by inhibiting the phosphorylation of P-38 and ERK in MAPK signaling pathway *in vivo*. Furthermore, EGFR may be a potential target for the treatment of acute lung injury, compound **6h** can be used as an anti-inflammatory potential candidate drug, for the treatment of ALI and related inflammatory diseases.

4. Experimental section

4.1. Chemistry

The reagents were purchased from commercial chemical reagent companies and used without further purification. Column chromatography was carried out on silica gel (200–300 mesh). ^{1}H NMR and ^{13}C NMR spectra were recorded on a 400 MHz spectrometer (Bruker Magnet System 400' 54 Ascend). Melting points were measured on a BUCHI B-540 and uncorrected. HRMS (ESI) was recorded using Agilent 6520 accurate-Mass Q-TOF LC/MS system (1200–6520/Agilent).

4.1.1. General procedure for preparation of compound **2** [9]

To a solution of 2,4-dichloropyrimidine (1.490 g, 10.0 mmol, 1.0 equiv.) and anhydrous aluminum chloride (1.333 g, 10.0 mmol, 1.0 equiv.) in ethylene glycol dimethyl ether (10 mL) and the suspension was stirred at room temperature for 5 min, followed by addition of 1-methylindole (1.312 g, 10.0 mmol, 1.0 equiv.). The mixture was heated to 80 °C for 2 h. The reaction mixture was cooled to room temperature and added into vigorously stirred water (50 mL) within 5 min. After the addition was complete, the mixture was stirred for 30 min, filtered, and the solid was washed with water (50 mL). The crude product was purified by column chromatography on silica gel to afford 1.342 g of compound **2** as a white solid in 55% yield.

*3-(2-Chloropyrimidin-*4-yl*)-1-methylindole (**2**):* white solid [12]; m.p. 199–200 °C; ^{1}H NMR (400 MHz, $CDCl_3$) δ 8.44 (d, J = 5.4 Hz, 1H), 8.36–8.32 (m, 1H), 7.94 (s, 1H), 7.48 (d, J = 5.4 Hz, 1H), 7.43–7.38 (m, 1H), 7.37–7.37 (m, 2H), 3.88 (s, 3H).

4.1.2. General procedure for preparation of compound **3** [12]

3-(2-chloropyrimidin-4-yl)-1-methylindole (2.447 g, 10.0 mmol, 1.0 equiv.) and 4-fluoro-2-methoxy-5-nitroaniline (1.861 g, 10.0 mmol, 1.0 equiv.) were dissolved in 1,4-dioxane (50 mL) at room temperature, followed by addition of 4-methylbenzenesulfonic acid hydrate (2.283 g, 12.0 mmol, 1.2 equiv.). The resulting mixture was stirred at 105 °C for 4 h. The resulting solution was cooled to room temperature. After filtration, the solid cake was washed with CH_2Cl_2/EtOAc (V/V 1:3) and dried at 60 °C to afford compound **3** as a yellow solid, which was directly used into the next step.

4.1.3. General procedure for preparation of ***AZD-1***

Iron powder (0.168 g, 3.00 mmol, 6.0 equiv.) and ammonium chloride (0.020 g, 0.38 mmol, 0.75 equiv.) were add into a solution of compound **3** (0.197 g, 0.50 mmol, 1.0 equiv.) in ethanol/water (V/V = 3:1, 16 mL) and the reaction mixture was stirred at 100 °C for 4 h. The resulting mixture was cooled to room temperature, filtered, and concentrated under reduced pressure. The residue was dissolved in CH_2Cl_2 (30 mL) and washed by water, dried over anhydrous Na_2SO_4 and concentrated under reduced pressure. The residue was purified by column chromatography to obtain 0.154 g as a yellow liquid in 85% yield.

*4-Fluoro-6-methoxy-N^1-(4-(1-methyl-1H-indol-*3-yl*)pyrimidin-*2-yl*)benzene-1,3-diamine (**AZD-1**):* yellow oil; ^{1}H NMR (400 MHz, $CDCl_3$) δ 8.52–8.50 (m, 1H), 8.34 (d, J = 5.3 Hz, 1H), 8.29 (d, J = 9.8 Hz, 1H), 7.75 (s, 1H), 7.55 (s, 1H), 7.40–7.38 (m, 1H), 7.35–7.30 (m, 2H), 7.02 (d, J = 5.3 Hz, 1H), 6.68 (d, J = 11.9 Hz, 1H), 3.86 (s, 6H), 3.54 (s, 2H). ^{13}C NMR (100 MHz, $CDCl_3$) δ 162.3, 160.0, 157.1, 146.1 ($J_{C\text{-}F}$ = 232.2 Hz), 141.0 ($J_{C\text{-}F}$ = 8.3 Hz), 138.0, 131.2, 126.9 ($J_{C\text{-}F}$ = 13.2 Hz), 126.02, 125.99 ($J_{C\text{-}F}$ = 2.9 Hz), 122.7, 122.0, 121.3, 114.1, 109.9, 108.8 ($J_{C\text{-}F}$ = 3.3 Hz), 108.0, 99.7 ($J_{C\text{-}F}$ = 23.9 Hz), 56.5, 33.3. HRMS(ESI): calcd. for $C_{20}H_{19}FN_5ONa$ $[M+Na]^+$ 386.1388; found 386.1388.

4.1.4. General procedure for preparation of ***4a-h***

To a solution of compound **3** (0.787 g, 2.0 mmol, 1.0 equiv.) and various secondary amines (2.4 mmol, 1.2 equiv.) in dimethyl sulfoxide (6 mL), followed by potassium carbonate (0.415 g, 3.0 mmol, 1.5 equiv.). The resulting mixture was stirred at 90 °C for 8 h. The resulting mixture was cooled to room temperature, followed by addition of H_2O (15 mL). After extraction with CH_2Cl_2 (3 × 40 mL), the combined organic layer was washed with brine and dried over anhydrous Na_2SO_4, filtered, and concentrated under reduced pressure. The crude product was purified by column chromatography on silica gel to obtain the desired products **4a**-**h** in 60–89% yield.

*4.1.4.1. N^1,N^1-diethyl-5-methoxy-N4-(4-(1-methyl-1H-indol-3-yl) pyrimidin-2-yl)-2-nitrobenzene-1,4-diamine (**4a**).* Red solid, m.p. 194–196 °C. ^{1}H NMR (500 MHz, $CDCl_3$) δ 9.50 (s, 1H), 8.38 (s, 1H), 8.20 (s, 2H), 7.58 (s, 1H), 7.38 (s, 1H), 7.31 (s, 2H), 7.17 (s, 1H), 6.64 (s,

1H), 3.97 (s, 3H), 3.91 (s, 3H), 3.19 (s, 4H), 1.14 (s, 6H). ^{13}C NMR (100 MHz, $CDCl_3$) δ 161.9, 159.2, 157.9, 151.7, 140.9, 138.1, 137.2, 133.1, 125.8, 124.3, 122.4, 121.4, 120.8, 115.8, 113.7, 110.2, 108.3, 103.9, 56.1, 47.4, 33.5, 12.8. HRMS(ESI): calcd. for $C_{24}H_{27}N_6O_3$ $[M+H]^+$ 447.2139; found 447.2128.

*4.1.4.2. N^1,N^1-dibutyl-5-methoxy-N^4-(4-(1-methyl-1H-indol-3-yl) pyrimidin-2-yl)-2-nitrobenzene-1,4-diamine (**4b**).* Red solid, m.p. 164–165 °C. ^{1}H NMR (400 MHz, $CDCl_3$) δ 9.51 (s, 1H), 8.36 (d, J = 5.3 Hz, 1H), 8.23 (s, 1H), 8.16–8.14 (m, 1H), 7.56 (s, 1H), 7.38 (d, J = 8.5 Hz, 1H), 7.32–7.26 (m, 2H), 7.16 (d, J = 5.3 Hz, 1H), 6.60 (s, 1H), 3.96 (s, 3H), 3.91 (s, 3H), 3.12 (t, J = 7.3 Hz, 4H), 1.52 (p, J = 7.3 Hz, 4H), 1.33–1.25 (m, 4H), 0.89 (t, J = 7.3 Hz, 6H). ^{13}C NMR (100 MHz, $CDCl_3$) δ 161.8, 159.3, 157.9, 151.9, 141.8, 138.1, 136.0, 133.1, 125.8, 123.7, 122.4, 121.3, 120.7, 116.0, 113.7, 110.2, 108.2, 103.6, 56.0, 53.0, 33.5, 29.7, 20.3, 14.0. HRMS(ESI): calcd. for $C_{28}H_{35}N_6O_3$ $[M+H]^+$ 503.2765; found 503.2765.

*4.1.4.3. N-(2-methoxy-5-nitro-4-(pyrrolidin-1-yl)phenyl)-4-(1-methyl-1H-indol-3-yl)pyrimidin-2-amine (**4c**).* Red solid, m.p. 242–245 °C. ^{1}H NMR (400 MHz, $CDCl_3$) δ 9.51 (s, 1H), 8.34 (d, J = 25.2 Hz, 2H), 8.16 (d, J = 7.1 Hz, 1H), 7.45–7.40 (m, 2H), 7.30 (s, 2H), 7.17 (d, J = 5.3 Hz, 1H), 6.37 (s, 1H), 3.98 (s, 3H), 3.95 (s, 3H), 3.28 (s, 4H), 2.02 (s, 4H). ^{13}C NMR (100 MHz, $CDCl_3$) δ 161.8, 159.4, 157.9, 152.9, 140.7, 138.1, 133.2, 129.7, 122.3, 121.3, 120.7, 120.3, 117.1, 115.8, 113.8, 110.2, 107.9, 96.3, 55.9, 51.0, 33.5, 25.8. HRMS(ESI): calcd. for $C_{24}H_{25}N_6O_3$ $[M+H]^+$ 445.1983; found 445.1982.

*4.1.4.4. N-(2-methoxy-5-nitro-4-(piperidin-1-yl)phenyl)-4-(1-methyl-1H-indol-3-yl)pyrimidin-2-amine (**4d**).* Red solid, m.p. 210–212 °C. ^{1}H NMR (400 MHz, $CDCl_3$) δ 9.65 (s, 1H), 8.39 (d, J = 5.3 Hz, 1H), 8.30 (s, 1H), 8.17–8.15 (m, 1H), 7.55 (s, 1H), 7.42–7.39 (m, 1H), 7.33–7.30 (m, 2H), 7.19 (d, J = 5.3 Hz, 1H), 6.58 (s, 1H), 3.99 (s, 3H), 3.93 (s, 3H), 3.05 (t, J = 5.2 Hz, 4H), 1.80 (q, J = 5.7 Hz, 4H), 1.64 (d, J = 6.0 Hz, 2H). ^{13}C NMR (100 MHz, $CDCl_3$) δ 161.8, 159.2, 157.9, 152.4, 144.3, 138.1, 134.8, 133.2, 125.8, 123.9, 122.3, 121.3, 120.7, 116.5, 113.6, 110.2, 108.2, 101.6, 56.1, 53.8, 33.5, 26.1, 24.2. HRMS(ESI): calcd. for $C_{25}H_{27}N_6O_3$ $[M+H]^+$ 459.2139; found 459.2121.

4.1.4.5 *N*-(4-(azepan-1-yl)-2-methoxy-5-nitrophenyl)-4-(1-methyl-1H-indol-3-yl)pyrimidin-2-amine (**4e**):

Red solid, m.p. 194–196 °C. ^{1}H NMR (500 MHz, $CDCl_3$) δ 9.45 (s, 1H), 8.36 (d, J = 5.2 Hz, 1H), 8.24 (s, 1H), 8.17–8.15 (m, 1H), 7.47 (s, 1H), 7.39–7.37 (m, 1H), 7.32–7.29 (m, 2H), 7.15 (d, J = 5.0 Hz, 1H), 6.51 (s, 1H), 3.95 (s, 3H), 3.91 (s, 3H), 3.34–3.32 (m, 4H), 1.83 (s, 4H), 1.65 (d, J = 3.5 Hz, 4H). ^{13}C NMR (100 MHz, $CDCl_3$) δ 161.8, 159.3, 157.9, 152.5, 143.4, 138.1, 133.1, 131.6, 125.8, 122.3, 121.3, 121.3, 120.7, 116.8, 113.7, 110.1, 108.0, 99.7, 55.9, 53.0, 33.5, 28.3. HRMS(ESI): calcd. for $C_{26}H_{29}N_6O_3$ $[M+H]^+$ 473.2296; found 473.2279.

*4.1.4.5. N-(2-methoxy-4-(4-methylpiperazin-1-yl)-5-nitrophenyl)-4-(1-methyl-1H-indol-3-yl)pyrimidin-2-amine (**4f**).* Red solid, m.p. 207–208 °C. ^{1}H NMR (500 MHz, $CDCl_3$) δ 9.63 (s, 1H), 8.37 (d, J = 5.3 Hz, 1H), 8.24 (s, 1H), 8.15–8.13 (m, 1H), 7.54 (s, 1H), 7.39–7.37 (m, 1H), 7.32–7.28 (m, 2H), 7.17 (d, J = 5.3 Hz, 1H), 6.59 (s, 1H), 3.97 (s, 3H), 3.91 (s, 3H), 3.12 (t, J = 4.8 Hz, 4H), 2.64 (t, J = 4.7 Hz, 4H), 2.39 (s, 3H). ^{13}C NMR (100 MHz, $CDCl_3$) δ 161.8, 159.1, 157.9, 152.2, 142.8, 138.1, 135.5, 133.1, 125.7, 124.7, 122.3, 121.3, 120.7, 116.3, 113.6, 110.2, 108.3, 101.6, 56.1, 55.1, 52.3, 46.1, 33.4. HRMS(ESI): calcd. for $C_{25}H_{28}N_7O_3$ $[M+H]^+$ 474.2248; found 474.2229.

*4.1.4.6. N-(2-methoxy-4-morpholino-5-nitrophenyl)-4-(1-methyl-1H-indol-3-yl)pyrimidin-2-amine (**4g**).* Red solid, m.p. 207–209 °C. ^{1}H NMR (400 MHz, DMSO-d_6) δ 8.85 (s, 1H), 8.41–8.34 (m, 3H), 8.17 (s, 1H), 7.53 (d, J = 8.2 Hz, 1H), 7.25 (d, J = 6.3 Hz, 2H), 7.14 (t, J = 7.6 Hz, 1H), 6.89 (s, 1H), 4.00 (s, 3H), 3.88 (s, 3H), 3.77 (t, J = 4.3 Hz, 4H), 3.09 (t, J = 4.4 Hz, 4H). ^{13}C NMR (100 MHz, DMSO-d_6) δ 162.6, 160.3, 157.6, 155.1, 143.9, 138.1, 134.9, 133.6, 125.9, 124.1, 122.7, 122.4, 121.4, 119.1, 112.7, 110.9, 108.2, 103.7, 66.7, 57.0, 52.5, 33.6. HRMS(ESI): calcd. for $C_{24}H_{25}N_6O_4$ $[M+H]^+$ 461.1932; found 461.1935.

*4.1.4.7. N^1-(2-(dimethylamino)ethyl)-5-methoxy-N^1-methyl-N^4-(4-(1-methyl-1H-indol-3-yl)pyrimidin-2-yl)-2-nitrobenzene-1,4-diamine (**4h**).* Red solid, m.p. 117–119 °C; ^{1}H NMR (400 MHz, DMSO-d_6) δ 8.66 (s, 1H), 8.36 (d, J = 8.0 Hz, 1H), 8.32–8.31 (m, 2H), 8.09 (s, 1H), 7.51 (d, J = 8.2 Hz, 1H), 7.27–7.25 (m, 1H), 7.21 (d, J = 5.4 Hz, 1H), 7.14–7.10 (m, 1H), 6.84 (s, 1H), 3.95 (s, 3H), 3.87 (s, 3H), 3.26 (t, J = 6.9 Hz, 2H), 2.85 (s, 3H), 2.48 (t, J = 6.4 Hz, 2H), 2.16 (s, 6H). ^{13}C NMR (100 MHz, DMSO-d_6) δ 162.6, 160.5, 157.6, 155.3, 144.3, 138.1, 133.5, 132.6, 125.9, 122.7, 122.5, 121.8, 121.3, 119.8, 112.8, 110.9, 107.8, 102.5, 56.8, 56.8, 53.3, 45.9, 41.0, 33.5. HRMS(ESI): calcd. for $C_{25}H_{29}N_7O_3Na$ $[M+Na]^+$ 498.2224; found 498.2223.

*4.1.5. General procedure for preparation of **5a-h***

Iron powder (0.168 g, 3.0 mmol, 6.0 equiv.) and ammonium chloride (0.020 g, 0.38 mmol, 0.75 equiv.) were add into a solution of **4a-h** (0.5 mmol, 1.0 equiv.) in ethanol/water (V/V = 3:1, 16 mL). The reaction mixture was stirred at 100 °C for 4 h and cooled to room temperature. After filtration and concentration under reduced pressure, the residue was dissolved in CH_2Cl_2 (30 mL) and washed with water. The organic phase was dried over anhydrous Na_2SO_4 and concentrated under reduced pressure. The residue was purified by column chromatography on silica gel to obtain a yellow liquid in 51–95% yield.

*4.1.5.1. N^1,N^1-diethyl-5-methoxy-N^4-(4-(1-methyl-1H-indol-3-yl) pyrimidin-2-yl)benzene-1,2,4-triamine (**5a**).* Yellow oil; ^{1}H NMR (400 MHz, $CDCl_3$) δ 8.56–8.53 (m, 1H), 8.33 (d, J = 5.3 Hz, 1H), 8.24 (s, 1H), 7.69 (d, J = 2.1 Hz, 2H), 7.34–7.31 (m, 3H), 6.96 (d, J = 5.3 Hz, 1H), 6.74 (s, 1H), 4.01 (s, 2H), 3.88 (s, 3H), 3.74 (s, 3H), 2.99 (q, J = 7.1 Hz, 4H), 1.07 (t, J = 7.1 Hz, 6H). ^{13}C NMR (100 MHz, $CDCl_3$) δ 162.3, 160.2, 157.1, 141.3, 138.4, 137.9, 131.3, 129.9, 127.0, 126.0, 122.6, 122.1, 121.2, 114.1, 109.8, 107.7, 106.9, 106.5, 56.8, 48.7, 33.2, 13.0. HRMS(ESI): calcd. for $C_{24}H_{28}N_6ONa$ $[M+Na]^+$ 439.2217; found 439.2217.

*4.1.5.2. N^1,N^1-dibutyl-5-methoxy-N^4-(4-(1-methyl-1H-indol-3-yl) pyrimidin-2-yl)benzene-1,2,4-triamine (**5b**).* Yellow oil; ^{1}H NMR (400 MHz, $CDCl_3$) δ 8.54 (dd, J = 6.4, 2.9 Hz, 1H), 8.33 (d, J = 5.3 Hz, 1H), 8.23 (s, 1H), 7.71 (s, 1H), 7.69 (s, 1H), 7.37–7.30 (m, 3H), 6.98 (d, J = 5.3 Hz, 1H), 6.77 (s, 1H), 3.94 (s, 2H), 3.89 (s, 3H), 3.77 (s, 3H), 2.94–2.90 (m, 4H), 1.53–1.45 (m, 4H), 1.42–1.33 (m, 4H), 0.95 (t, J = 7.2 Hz, 6H). ^{13}C NMR (100 MHz, $CDCl_3$) δ 162.3, 160.2, 157.1, 141.3, 138.1, 138.0, 131.3, 130.95, 127.0, 126.1, 122.6, 122.1, 121.2, 114.1, 109.8, 107.7, 106.9, 106.6, 56.8, 54.9, 33.2, 29.9, 20.7, 14.2. HRMS(ESI): calcd. for $C_{28}H_{36}N_6ONa$ $[M+Na]^+$ 495.2843; found 495.2845.

*4.1.5.3. 6-Methoxy-N^1-(4-(1-methyl-1H-indol-3-yl)pyrimidin-2-yl)-4-(pyrrolidin-1-yl)benzene-1,3-diamine (**5c**).* Yellow oil; ^{1}H NMR (400 MHz, $CDCl_3$) δ 8.55–8.52 (m, 1H), 8.34 (d, J = 5.3 Hz, 1H), 8.17 (s, 1H), 7.81 (s, 1H), 7.58 (s, 1H), 7.42–7.39 (m, 1H), 7.36–7.30 (m, 2H), 7.02 (d, J = 5.3 Hz, 1H), 6.73 (s, 1H), 3.90 (s, 3H), 3.88 (s, 3H), 3.09–3.06 (m, 4H), 1.99–1.95 (m, 4H). ^{13}C NMR (100 MHz, $CDCl_3$) δ 162.3, 160.2, 157.2, 141.4, 138.0, 135.2, 131.1, 131.0, 126.1, 125.7, 122.6, 122.1, 121.3, 114.3, 109.8, 107.7, 107.6, 103.4, 56.9, 51.4, 33.4, 24.1. HRMS(ESI): calcd. for $C_{24}H_{26}N_6ONa$ $[M+Na]^+$ 437.2060; found 437.2060.

*4.1.5.4. 6-Methoxy-N^1-(4-(1-methyl-1H-indol-3-yl)pyrimidin-2-yl)-4-(piperidin-1-yl)benzene-1,3-diamine (**5d**).* Yellow oil; ^{1}H NMR (400 MHz, $CDCl_3$) δ 8.59–8.56 (m, 1H), 8.33 (d, J = 5.3 Hz, 1H), 8.24 (s, 1H), 7.67 (d, J = 10.5 Hz, 2H), 7.35–7.29 (m, 3H), 6.96 (d, J = 5.3 Hz, 1H), 6.75 (s, 1H), 3.90 (s, 3H), 3.76 (s, 3H), 2.92–2.89 (m, 4H), 1.81–1.75 (m, 4H), 1.64 (s, 2H). ^{13}C NMR (100 MHz, $CDCl_3$) δ 162.3, 160.2, 157.1, 141.3, 137.9, 135.3, 134.2, 131.3, 126.3, 126.1, 122.6, 122.2, 121.2, 114.1, 109.8, 107.6, 107.2, 104.3, 56.8, 53.2, 33.2, 27.0, 24.5. HRMS(ESI): calcd. for $C_{25}H_{28}N_6ONa$ $[M+Na]^+$ 451.2217; found 451.2217.

*4.1.5.5. 4-(Azepan-1-yl)-6-methoxy-N^1-(4-(1-methyl-1H-indol-3-yl) pyrimidin-2-yl)benzene-1,3-diamine (**5e**).* Yellow oil; ^{1}H NMR (400 MHz, $CDCl_3$) δ 8.54–8.52 (m, 1H), 8.34 (d, J = 5.4 Hz, 1H), 8.17 (s, 1H), 7.79 (s, 1H), 7.60 (s, 1H), 7.41–7.38 (m, 1H), 7.37–7.31 (m, 2H), 7.02 (d, J = 5.3 Hz, 1H), 6.73 (s, 1H), 3.93 (s, 2H), 3.88 (s, 3H), 3.87 (s, 3H), 3.07 (t, J = 5.5 Hz, 4H), 1.86–1.75 (m, 8H). ^{13}C NMR (100 MHz, $CDCl_3$) δ 162.2, 160.2, 157.2, 141.3, 137.9, 136.1, 135.5, 131.2, 126.2, 126.1, 122.6, 122.1, 121.3, 114.3, 109.8, 107.7, 107.0, 106.1, 56.8, 56.2, 33.3, 30.0, 27.1. HRMS(ESI): calcd. for $C_{26}H_{30}N_6ONa$ $[M+Na]^+$ 465.2373; found 465.2373.

*4.1.5.6. 6-Methoxy-N^1-(4-(1-methyl-1H-indol-3-yl)pyrimidin-2-yl)-4-(4-methylpiperazin-1-yl)benzene-1,3-diamine (**5f**).* Yellow oil; ^{1}H NMR (400 MHz, $CDCl_3$) δ 8.54–8.51 (m, 1H), 8.34 (d, J = 5.3 Hz, 1H), 8.20 (s, 1H), 7.77 (s, 1H), 7.61 (s, 1H), 7.40–7.38 (m, 1H), 7.36–7.30 (m, 2H), 7.01 (d, J = 5.3 Hz, 1H), 6.74 (s, 1H), 3.87 (s, 3H), 3.86 (s, 3H), 2.98 (t, J = 4.7 Hz, 4H), 2.62 (s, 4H), 2.39 (s, 3H). ^{13}C NMR (100 MHz, $CDCl_3$) δ 162.3, 160.1, 157.1, 141.3, 137.9, 135.3, 132.4, 131.1, 126.7, 126.0, 122.6, 122.1, 121.3, 114.2, 109.8, 107.7, 107.1, 104.3, 56.8, 56.0, 51.5, 46.30, 33.3. HRMS(ESI): calcd. for $C_{25}H_{29}N_7ONa$ $[M+Na]^+$ 466.2326; found 465.2325.

*4.1.5.7. 6-Methoxy-N^1-(4-(1-methyl-1H-indol-3-yl)pyrimidin-2-yl)-4-morpholinobenzene-1,3-diamine (**5g**).* Yellow oil; ^{1}H NMR (400 MHz, $CDCl_3$) δ 8.56–8.53 (m, 1H), 8.34 (d, J = 5.3 Hz, 1H), 8.23 (s, 1H), 7.77 (d, J = 1.9 Hz, 1H), 7.63 (s, 1H), 7.40–7.38 (m, 1H), 7.36–7.30 (m, 2H), 7.01 (d, J = 5.3 Hz, 1H), 6.71 (s, 1H), 3.91 (s, 2H), 3.89 (s, 6H), 3.85 (s, 4H), 2.95 (t, J = 4.5 Hz, 4H). ^{13}C NMR (100 MHz, $CDCl_3$) δ 162.3, 160.1, 157.1, 141.3, 138.0, 135.3, 132.1, 131.2, 126.9, 126.1, 122.7, 122.1, 121.3, 114.2, 109.8, 107.8, 107.2, 104.1, 67.8, 56.8, 52.0, 33.3. HRMS(ESI): calcd. for $C_{24}H_{26}N_6O_2Na$ $[M+Na]^+$ 453.2009; found 453.2010.

*4.1.5.8. N^1-(2-(dimethylamino)ethyl)-5-methoxy-N^1-methyl-N^4-(4-(1-methyl-1H-indol-3-yl)pyrimidin-2-yl)benzene-1,2,4-triamine (**5h**).* Yellow oil; ^{1}H NMR (400 MHz, DMSO-d_6) δ 8.52 (dd, J = 7.1, 1.9 Hz, 1H), 8.33 (d, J = 5.3 Hz, 1H), 8.27 (s, 1H), 7.91 (s, 1H), 7.72 (s, 1H), 7.48 (d, J = 8.8 Hz, 1H), 7.29–7.21 (m, 2H), 7.17 (d, J = 5.4 Hz, 1H), 6.80 (s, 1H), 4.53 (s, 2H), 3.85 (s, 3H), 3.79 (s, 3H), 2.95 (t, J = 6.5 Hz, 2H), 2.65 (s, 3H), 2.48 (t, J = 6.6 Hz, 2H), 2.26 (s, 6H). ^{13}C NMR (100 MHz, DMSO-d_6) δ 162.6, 160.8, 157.5, 141.9, 138.1, 137.4, 133.5, 133.2, 126.1, 126.0, 122.7, 122.6, 121.4, 113.0, 110.7, 109.2, 107.4, 105.6, 57.4, 56.9, 54.0, 45.7, 42.1, 33.4. HRMS(ESI): calcd. for $C_{25}H_{31}N_7ONa$ $[M+Na]^+$ 468.2482; found 468.2485.

*4.1.6. General procedure for preparation of **6a-h***

To a solution of **5a-h** in dichloromethane, followed by excess saturated HCl/EtOH solution. The reaction mixture was stirred at room temperature for 3 h, and the resulting solution was concentrated under reduced pressure to obtain a yellow solid.

*4.1.7. General procedure for preparation of **7a-b***

To a solution of compound **5h** (4.456 g, 10.0 mmol, 1.0 equiv.) in dichloromethane (25 mL), various acyl chloride (12.0 mmol, 1.2 equiv.) was added dropwise under argon at 0 °C. The reaction mixture was stirred at room temperature for 1 h. The resulting solution was filtered, the filter cake was washed with ethyl acetate, and dried to obtain **7a-b** as a yellow solid, which was directly used into the next step.

*4.1.7.1. 2-Chloro-N-(2-((2-(dimethylamino)ethyl) (methyl)amino)-4-methoxy-5-((4-(1-methyl-1H-indol-3-yl)pyrimidin-2-yl)amino) phenyl)acetamide (**7a**).* Yellow solid; m.p. 242–244 °C. ^{1}H NMR (500 MHz, $CDCl_3$) δ 10.30 (s, 1H), 9.71 (s, 1H), 8.93 (s, 1H), 8.39 (d, J = 5.3 Hz, 1H), 8.09 (dd, J = 7.0, 1.8 Hz, 1H), 7.74 (s, 1H), 7.42–7.40 (m, 1H), 7.31 (dd, J = 7.1, 1.4 Hz, 1H), 7.29 (d, J = 1.8 Hz, 1H), 7.22 (d, J = 5.3 Hz, 1H), 6.81 (s, 1H), 4.25 (s, 2H), 4.00 (s, 3H), 3.91 (s, 3H), 3.00 (t, J = 6.3 Hz, 2H), 2.71 (s, 3H), 2.39 (d, J = 6.3 Hz, 2H), 2.31 (s, 6H). HRMS(ESI): calcd. for $C_{27}H_{33}ClN_7O_2$ $[M+H]^+$ 522.2379; found 522.2376.

*4.1.7.2. 4-Chloro-N-(2-((2-(dimethylamino)ethyl) (methyl)amino) -4-methoxy-5-((4-(1-methyl-1H-indol-3-yl)pyrimidin-2-yl)amino) phenyl) butanamide (**7b**).* Yellow solid; m.p. 250–252 °C. ^{1}H NMR (400 MHz, D_2O) δ 7.62 (s, 1H), 7.23 (s, 1H), 7.15 (s, 1H), 6.92–6.87 (m, 2H), 6.84–6.66 (m, 4H), 3.72 (s, 3H), 3.45 (t, J = 6.4 Hz, 2H), 3.25 (s, 4H), 2.95 (s, 3H), 2.77 (s, 8H), 2.46 (q, J = 8.1 Hz, 6H). HRMS(ESI): calcd. for $C_{29}H_{37}ClN_7O_2$ $[M+H]^+$ 550.2692; found 550.2692.

*4.1.8. General procedure for preparation of **8a-b***

To a solution of compound **7** (5.0 mmol, 1.0 equiv.) in *N,N*-dimethylformamide (15 mL) was added NaN_3 (2.5 mmol, 2.5 equiv.). The reaction mixture was stirred at 90 °C for 8 h. The resulting solution was cooled to room temperature, and the resulting mixture was diluted with H_2O (15 mL) and extracted with CH_2Cl_2. The combined organic layers were washed with brine and dried over anhydrous Na_2SO_4, filtered, and concentrated under reduced pressure. The crude product was purified by column chromatography to obtain **8a-b** as a yellow solid in 56–69% yield.

*4.1.8.1. 2-Azido-N-(2-((2-(dimethylamino)ethyl) (methyl)amino) -4-methoxy-5-((4-(1-methyl-1H-indol-3-yl)pyrimidin-2-yl)amino) phenyl)acetamide (**8a**).* Yellow solid; m.p. 118–120 °C; ^{1}H NMR (500 MHz, $CDCl_3$): δ 10.22 (s, 1H), 9.67 (s, 1H), 8.92 (s, 1H), 8.39 (d, J = 5.3 Hz, 1H), 8.10 (d, J = 7.4 Hz, 1H), 7.75 (s, 1H), 7.41 (d, J = 7.5 Hz, 1H), 7.31–7.25 (m, 2H), 7.21 (d, J = 5.3 Hz, 1H), 6.80 (s, 1H), 4.05 (s, 2H), 4.00 (s, 3H), 3.99 (s, 3H), 2.94 (t, J = 5.9 Hz, 2H) 2.70 (s, 3H), 2.30 (t, J = 6.0 Hz, 2H), 2.27 (s, 6H). ^{13}C NMR (125 MHz, $CDCl_3$): δ 164.1, 162.1, 159.6, 157.8, 144.6, 138.2, 134.67, 134.64, 128.5, 127.7, 125.9, 121.8, 120.9, 120.3, 113.6, 110.1, 109.8, 108.0, 104.5, 57.4, 56.1, 55.9, 53.3, 45.4, 44.2, 33.0. HRMS(ESI): calcd. for $C_{27}H_{32}N_{10}O_2Na$ $[M+Na]^+$ 551.2602; found 551.2604.

*4.1.8.2. 4-Azido-N-(2-((2-(dimethylamino)ethyl) (methyl)amino) -4-methoxy-5-((4-(1-methyl-1H-indol-3-yl)pyrimidin-2-yl)amino) phenyl)butanamide (**8b**).* Yellow solid; m.p. 164–166 °C. ^{1}H NMR (500 MHz, $CDCl_3$) δ 10.06 (s, 1H), 9.69 (s, 1H), 8.98 (s, 1H), 8.39 (d, J = 5.2 Hz, 1H), 8.11 (dd, J = 7.1, 1.9 Hz, 1H), 7.73 (s, 1H), 7.45–7.36 (m, 1H), 7.32–7.26 (m, 2H), 7.21 (d, J = 5.3 Hz, 1H), 6.80 (s, 1H), 3.99 (s, 3H), 3.89 (s, 3H), 3.46 (t, J = 6.7 Hz, 2H), 2.92–2.88 (m, 2H), 2.70 (s, 3H), 2.53 (t, J = 7.3 Hz, 2H), 2.29–2.27 (m, 8H), 2.12–2.07 (m, 2H). ^{13}C NMR (125 MHz, $CDCl_3$): δ 169.2, 162.1, 159.6, 157.8, 144.1, 138.2, 134.7, 134.2, 129.6, 127.7, 125.9, 121.8, 120.9, 120.4, 113.7, 110.0, 109.8, 107.9, 104.7, 57.3, 56.1, 51.0, 45.3, 44.0, 34.1, 33.0, 25.0. HRMS(ESI): calcd. for $C_{29}H_{36}N_{10}O_2Na$ $[M+Na]^+$ 579.2915; found 579.2916.

4.2. Animals

Male C57BL/6 mice of 20–25 g were obtained from the Shanghai

Laboratory Animal Center (CAS). The mice were kept in standard conditions and maintained in specific pathogen-free conditions under a 12 h light-dark cycle at 25 °C, with free access to diet and water. All animal care and experimental procedures were approved by the Experimental Animal Center of Zhejiang Chinese Medical University (no. SYXK-2018-0012).

4.3. Cells and reagents

Lipopolysaccharide (LPS) was obtained from Shanghai yuan ye Bio-Technology Co., Ltd. (Shang hai, China). Saline was prepared as 0.9% NaCl solution. The human IL-6 enzyme-linked immunosorbent assay (ELISA) kit and human IL-8 ELISA kit were purchased from BioLegend, Inc. (San Diego, CA, USA). Human bronchial epithelial cells were obtained from the American Type Culture Collection (ATCC, U.S.). HBE cells were incubated in RPMI-1640 medium (Cienry, Huzhou, China) supplemented with 10% FBS (Every geen, Deqing, China) at 37 °C with 5% CO_2.

4.4. Determination of IL-6 and IL-8

The anti-inflammatory effects of new synthesized 4-indolyl-2-arylaminopyrimidine compounds were evaluated by inhibition of IL-6 and IL-8 release using in LPS stimulated HBE cells. After treatment of cells with indicated compounds and LPS, the IL-6 and IL-8 levels in medium were determined with an ELISA kit (Bio-Legend, San Diego, CA) according to the manufacturer's instructions. Briefly, cells were pretreated with 5 μM of indomethacin or prepared 4-indolyl-2-arylaminopyrimidine compounds for 30 min, then treated with LPS (100 μg/mL) for 24 h. After treatment, the culture media and cells were collected separately. The levels of IL-6 and IL-8 in the media were determined by ELISA. The total protein in cultural plates was collected and the concentrations were determined using BCA protein assay reagents. The total amount of the inflammatory factor in the media was normalized to the total protein amount of the viable cell.

4.5. MTT (methyl thiazolyl tetrazolium) assay

HBE were seeded into 96-well plates at a concentration of 1×10^4 cells per well in 1640 medium, supplemented with 10% FBS. After treatment with the compounds, cell were incubated with MTT (5 mg/mL) solution for 4 h at 37 °C in dark and dissolved in 100 μL of DMSO. Absorbance at 490 nm was detected by the multi-well-plate reader.

4.6. Real-time quantitative PCR

RNA was extracted from tissues using TRIZOL (Invitrogen; Thermo Fisher Scientific, Inc.). and then reverse transcribed into cDNA by the PrimeScript™ RT reagent Kit (Takara Bio, Inc.). Then, qPCR was performed with SYBR-Green (Bio-Rad Laboratories, Inc.) using the CFX96 Real-Time system (Bio-Rad Laboratories, Inc.). $2^{-\Delta\Delta Cq}$ method was used for the relative expression levels of mRNA. The primer sequences are shown as follows:

Mouse IL-1β forward: 5′-GAAATGCCACCTTTTGACAGTG-3′ and reverse , 5′-TGGATGCTCTCATCAGGACAG- 3′;

Mouse IL-6 forward: 5′-CTGCAAGAGACTTCCATCCAG-3′ and reverse , 5′-AGTGGTATAGACAGGTCTGTTGG- 3′;

Mouse TNF-α forward: 5′-CAGGCGGTGCCTATGTCTC-3′ and reverse , 5′-CGATCACCCCGAAGTTCAGTAG- 3′;

Mouse iNOS forward: 5′-GTTCTCAGCCCAACAATACAAGA-3′ and reverse , 5′-GTGGACGGGTCGATGTCAC- 3′;

Mouse GAPDH forward: 5′-AGGTCGGTGTGAACGGATTTG-3′ and reverse , 5′-GGGGTCGTTGATGGCAACA- 3′;

4.6.1. Animal model of ALI

Male C57BL/6 mice were randomly divided in four groups: control (n = 6), LPS (n = 6), **6h**-10 mg/kg + LPS (n = 6), **6h**-20 mg/kg + LPS (n = 6) and **6h**-20 mg/kg (n = 6). The mice were treated by intraperitoneal injection with 0.9% saline or **6h** for 3 days. As On the fourth day, after administration with 0.9% saline or **6h** for 1h, LPS (5 mg/kg) was then injected into the trachea. 18 h later, mice were killed.

4.7. Collection of bronchoalveolar lavage fluid (BALF)

The cold PBS (1 mL) was injected into lungs using a 2.5 mL syringe and repeated three times, the collected BALF was centrifuged at 4 °C and 800 g/min for 10 min. The supernatant was used for protein concentration measure by BCA protein assay kit (Beyotime Institute of Biotechnology). And the cell pellets obtained from BALF were washed and re-suspended in 10 mL PBS, total number of cells in BALF was counted.

4.8. Lung wet/dry weight ratio

Pulmonary edema was assessed by the lung wet/dry weight ratio. Mice were killed, and the lungs were removed and weighed (wet weight). Lungs were heated at 60 °C for 48 h until getting constant weight as dry weight, and calculate the W/D ratio.

4.9. Western blotting analysis

After treating the HBE cells with the drug for 24 h, wash them twice with pre-cooled PBS, add 5% protease inhibitor and 2% phosphatase inhibitor to the lysate (Beyotime Biotechnology) to collect cells, lyse the cells on ice for 30 min, centrifuge at 4 °C, 12000r/min, and 30min. Take the supernatant, which is the total cell protein. The amount of protein was quantitatively detected by the BCA method, and the protein was denatured at 100 °C for 5 min after diluting the protein with 5*x* protein loading buffer. The protein was separated by SDS-PAGE electrophoresis, transferred to membrane, blocked for 2h. Primary antibodies including GAPDH, β-tubulin, p-p38, p38, *p*-ERK, ERK, EGFR or p- EGFR (all obtained from Cell Signaling Technology) were incubated overnight at 4 °C. Wash the membrane with TBST, incubate with the secondary antibody 1:2000 for 2h, wash the membrane, and develop after chemiluminescence.

4.10. Histopathologic evaluation

Lung tissues were fixed in 4% paraformaldehyde solution, and embedded in paraffin, then cut into 5-μm-thick sections. The sections were stained with hematoxylin and eosin (H&E) staining. The stained cells were photographed for pathological analysis by a Nikon microscope (Nikon, Japan).

4.11. Statistical analysis

All data are expressed as mean ± standard error of the mean (SEM). Graphpad Prism 8 (GraphPad, San Diego, CA) was used for statistical analysis and graphing. Statistical analysis of results by the Student's t-test. P value less than 0.05 indicated that the difference

was statistically significant. ($p < 0.05$). All experiments were repeated at least three times.

Declaration of competing interest

The authors declare that they have no known competing financial interests or personal relationships that could have appeared to influence the work reported in this paper.

Acknowledgement

This work was supported by National Natural Science Foundation of China (21877099).

Appendix A. Supplementary data

Supplementary data to this article can be found online at https://doi.org/10.1016/j.ejmech.2021.113766.

References

[1] M. Chopra, J.S. Reuben, A.C. Sharma, Acute lung injury:apoptosis and signaling mechanisms, Exp. Biol. Med. 234 (2009) 361–371.
[2] W. Chen, X. Ge, F. Xu, Y. Zhang, Z. Liu, J. Pan, J. Song, Y. Dai, J. Zhou, J. Feng, G. Liang, Design, synthesis and biological evaluation of paralleled Aza resveratrol-chalcone compounds as potential anti-inflammatory agents for the treatment of acute lung injury, Bioorg. Med. Chem. Lett 25 (2015) 2998–3004.
[3] Y. Yatabe, K.M. Kerr, A. Utomo, P. Rajadurai, V.K. Tran, X. Du, T.Y. Chou, M.L. Enriquez, G.K. Lee, J. Iqbal, S. Shuangshoti, J.H. Chung, K. Hagiwara, Z. Liang, N. Normanno, K. Park, S. Toyooka, C.M. Tsai, P. Waring, L. Zhang, R. McCormack, M. Ratcliffe, Y. Itoh, M. Sugeno, T. Mok, EGFR mutation testing practices within the Asia Pacific region: results of a multicenter diagnostic survey, J. Thorac. Oncol. 10 (2015) 438–445.
[4] C. Harada, T. Kawaguchi, S. Ogata-Suetsugu, M. Yamada, N. Hamada, T. Maeyama, R. Souzaki, T. Tajiri, T. Taguchi, K. Kuwano, Y. Nakanishi, EGFR tyrosine kinase inhibition worsens acute lung injury in mice with repairing airway epithelium, Am. J. Respir. Crit. Care Med. 183 (2011) 743–751.
[5] S. Xiaoou, Z. Yali, C. Hongjin, D. Lili, H. Jie, L. Zhiguo, W. Wei, F. Zhiguo, L. Guang, Inhibition of epidermal growth factor receptor attenuates LPS induced inflammation and acute lung injury in rats, Oncotarget 8 (2017) 26648–26661.
[6] H. Tao, N. Li, Z. Zhang, H. Mu, C. Meng, H. Xia, L. Fu, Y. Xu, S. Zhang, Erlotinib protects LPS-induced acute lung injury in mice by inhibiting EGFR/TLR4 signaling pathway, Shock 51 (2019) 131–138.
[7] A. Elkamhawy, A.H.E. Hassan, S. Paik, Y. Sup Lee, H.H. Lee, J.S. Shin, K.T. Lee, E.J. Roh, EGFR inhibitors from cancer to inflammation: discovery of 4-fluoro-N-(4-(3-(trifluoromethyl)phenoxy)pyrimidin-5-yl)benzamide as a novel anti-inflammatory EGFR inhibitor, Bioorg. Chem. 86 (2019) 112–118.
[8] S. Sharma, D. Kumar, G. Singh, V. Monga, B. Kumar, Recent advancements in the development of heterocyclic anti-inflammatory agents, Eur. J. Med. Chem. 200 (2020) 112438.
[9] G. Maggiora, M. Vogt, D. Stumpfe, J. Bajorath, Molecular similarity in medicinal chemistry, J. Med. Chem. 57 (2013) 3186–3204.
[10] M. Gehringer, S.A. Laufer, Click chemistry: novel applications in cell biology and drug discovery, Angew Chem. Int. Ed. Engl. 56 (2017) 15504–15505.
[11] X. Jiang, X. Hao, L. Jing, G. Wu, D. Kang, X. Liu, P. Zhan, Recent applications of click chemistry in drug discovery, Expet Opin. Drug Discov. 14 (2019) 779–789.
[12] M.R. Finlay, M. Anderton, S. Ashton, P. Ballard, P.A. Bethel, M.R. Box, R.H. Bradbury, S.J. Brown, S. Butterworth, A. Campbell, C. Chorley, N. Colclough, D.A. Cross, G.S. Currie, M. Grist, L. Hassall, G.B. Hill, D. James, M. James, P. Kemmitt, T. Klinowska, G. Lamont, S.G. Lamont, N. Martin, H.L. McFarland, M.J. Mellor, J.P. Orme, D. Perkins, P. Perkins, G. Richmond, P. Smith, R.A. Ward, M.J. Waring, D. Whittaker, S. Wells, G.L. Wrigley, Discovery of a potent and selective EGFR inhibitor (AZD9291) of both sensitizing and T790M resistance mutations that spares the wild type form of the receptor, J. Med. Chem. 57 (2014) 8249–8267.
[13] D. Mokra, P. Kosutova, Biomarkers in acute lung injury, Respir. Physiol. Neurobiol. 209 (2015) 52–58.
[14] L.J. Cross, M.A. Matthay, Biomarkers in acute lung injury: insights into the pathogenesis of acute lung injury, Crit. Care Clin. 27 (2011) 355–377.
[15] H. Tunceroglu, A. Shah, J. Porhomayon, N.D. Nader, Biomarkers of lung injury in critical care medicine: past, present, and future, Immunol. Invest. 42 (2013) 247–261.
[16] T.C. Allen, A. Kurdowska, Interleukin 8 and acute lung injury, Arch. Pathol. Lab Med. 138 (2014) 266–269.
[17] K. Nepali, H.Y. Lee, J.P. Liou, Nitro-group-containing drugs, J. Med. Chem. 62 (2019) 2851–2893.
[18] Y. Zhang, D. Liang, L. Dong, X. Ge, F. Xu, W. Chen, Y. Dai, H. Li, P. Zou, S. Yang, G. Liang, Anti-inflammatory effects of novel curcumin analogs in experimental acute lung injury, Respir. Res. 16 (2015) 1–13.
[19] J. Qian, X. Chen, S. Shu, W. Zhang, B. Fang, X. Chen, Y. Zhao, Z. Liu, G. Liang, Design and synthesis novel di-carbonyl analogs of curcumin (DACs) act as potent anti-inflammatory agents against LPS-induced acute lung injury (ALI), Eur. J. Med. Chem. 167 (2019) 414–425.